Electronic Supplementary Material (ESI) for Journal of Materials Chemistry C.

Supporting information

Visualized Real-Time Flexible High-Temperature Sensing in Eu^{3+}/Tb^{3+}-doped $Y_2Mo_3O_{12}$ Negative Thermal Expansion Material Film

Shilei Yan[a]; *Dongming Pi[b]*; Yingzhu Zi[a]; Heping Zhao[a];Rongbao Feng[a];Keliang Ruan[a]; Jianbei Qiu[a];Zhiguo Song[a]; Anjun Huang[a]; Yue Liu[a];Yangke Cun[a]*;Zhengwen Yang[a]*;

[a]*College of Materials Science and Engineering, Kunming University of Science and Technology, Kunming, 650093, China;*

[b]*Yunnan North Photoelectric Instrument Co. Ltd., Kunming 650114, China*

* Corresponding author.

E-mail: cunyangke@kust.edu.cn;

E-mail:yangzw@kust.edu.cn;

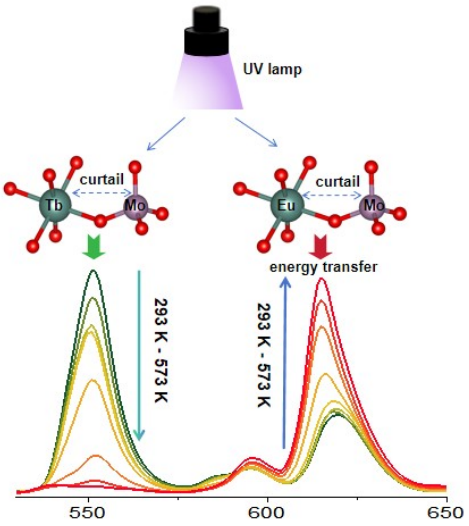

Fig S1. Visual temperature sensing mechanism diagram

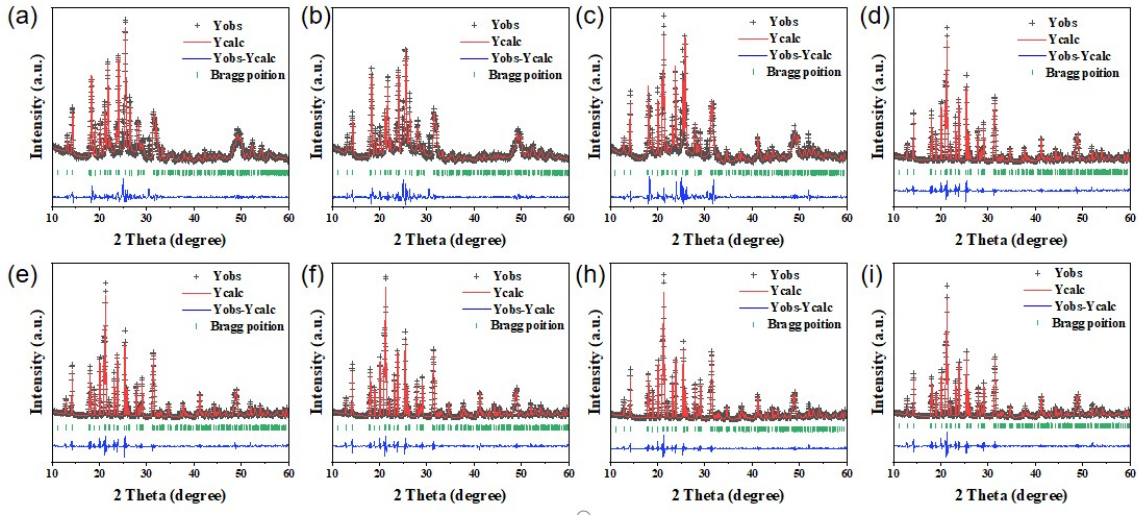

Fig S2. (a-i) The in-situ temperature-dependent refined XRD spectra of $Y_2Mo_3O_{12}$ at 293 K, 333 K, 373 K, 413 K, 453 K, 493 K, 533 K, 573 K, respectively.

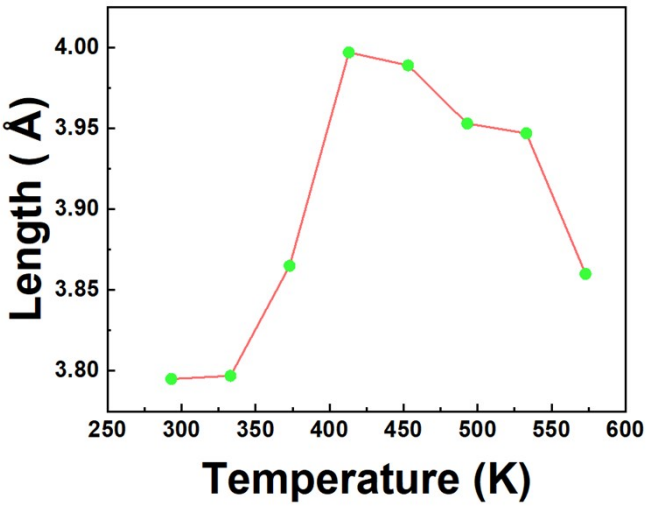

Fig S3. The ion distance between Y and Mo at 273 K-573 K

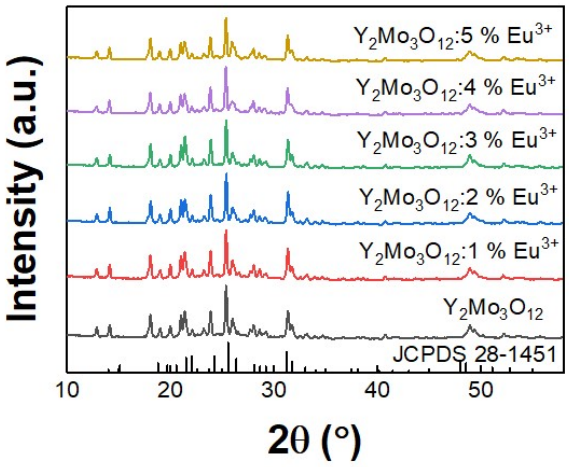

Fig S4. The XRD Spectra of $Y_2Mo_3O_{12}$: x% Eu^{3+} (x = 0,1,2,3,4,5)

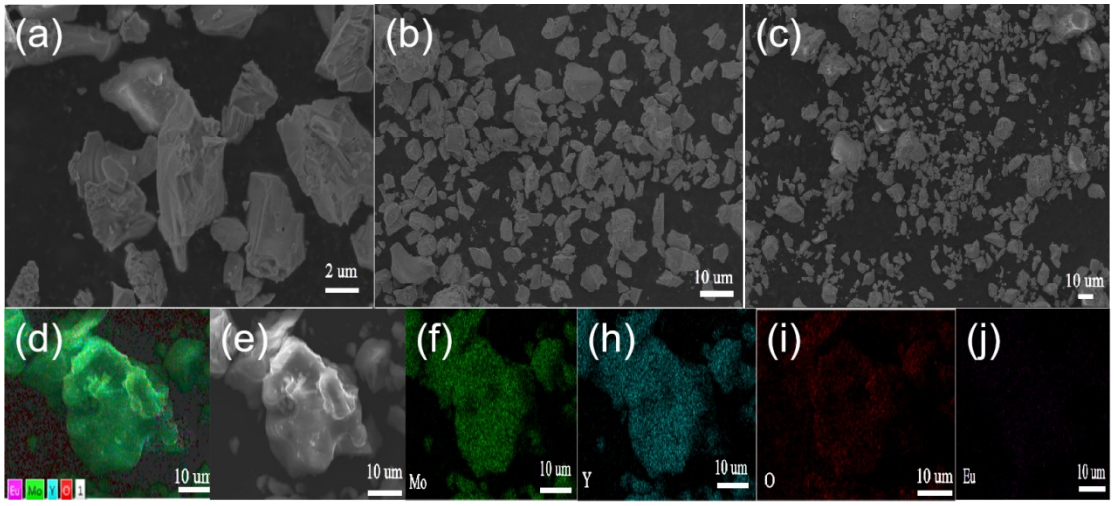

Fig S5. (a-c)The SEM with different magnification ratios of $Y_2Mo_3O_{12}$: 4% Eu^{3+} phosphor ; elemental mapping of Mo (f), Y(h), O (i) and Eu (j) elements

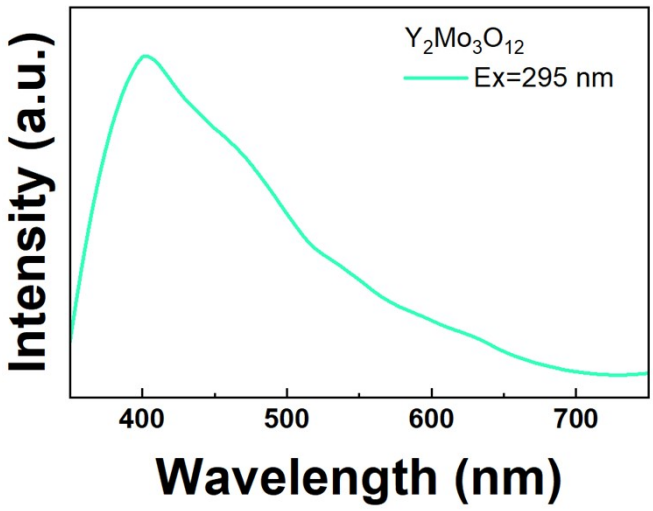

Fig S6. The PL spectrum of the $Y_2Mo_3O_{12}$ substrate

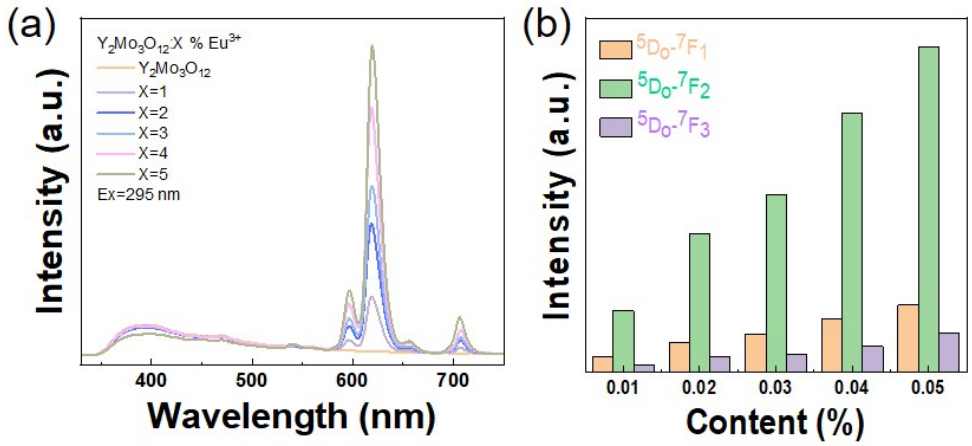

Fig S7. (a) The PL spectra and (b) integrated emission intensity of $Y_2Mo_3O_{12}$:x% Eu^{3+} (

x = 1,2,3,4,5) under 295 nm excitation

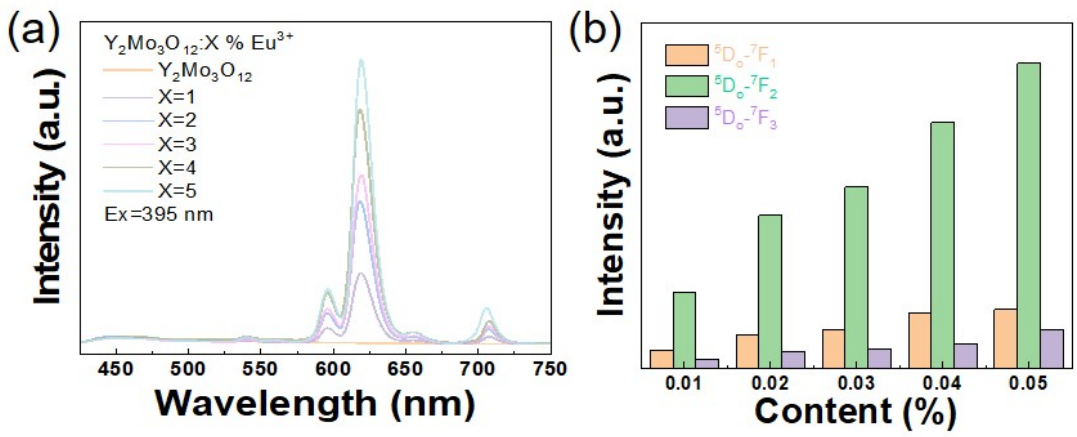

Fig S8. (a) The PL spectra and (b) integrated emission intensity of $Y_2Mo_3O_{12}$:x% Eu^{3+} (x = 1,2,3,4,5) under 395 nm excitation

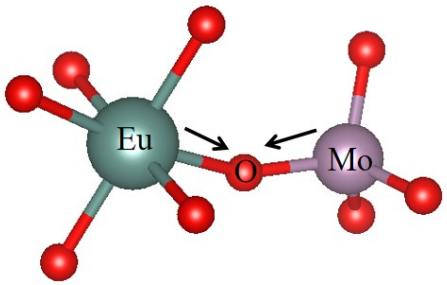

Fig S9. Thermal vibration diagram of Eu-O-Mo in $Y_2Mo_3O_{12}$: 4% Eu^{3+}

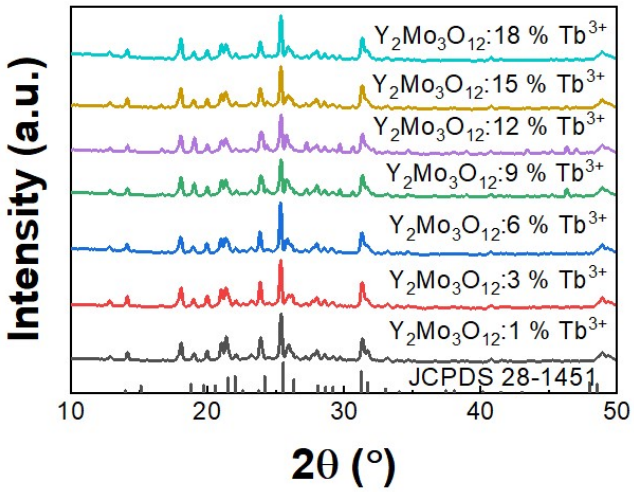

Fig S10. The XRD Spectra of $Y_2Mo_3O_{12}$: x% Tb^{3+} (x = 0,1,3,6,9,12,15,18)

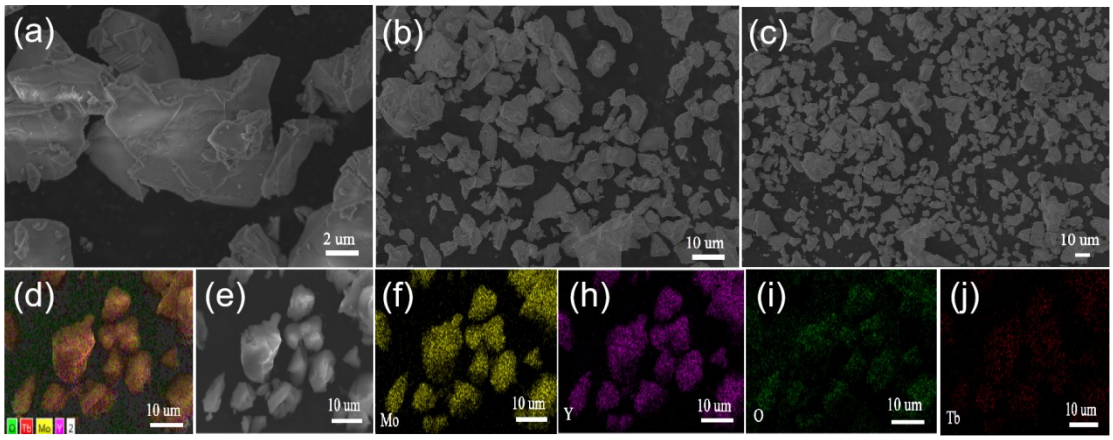

Fig S11. (a-c)The SEM with different magnification ratios of $Y_2Mo_3O_{12}$: 15%Tb^{3+} phosphor ; elemental mapping of Mo (f), Y(h), O (i) and Tb (j) elements

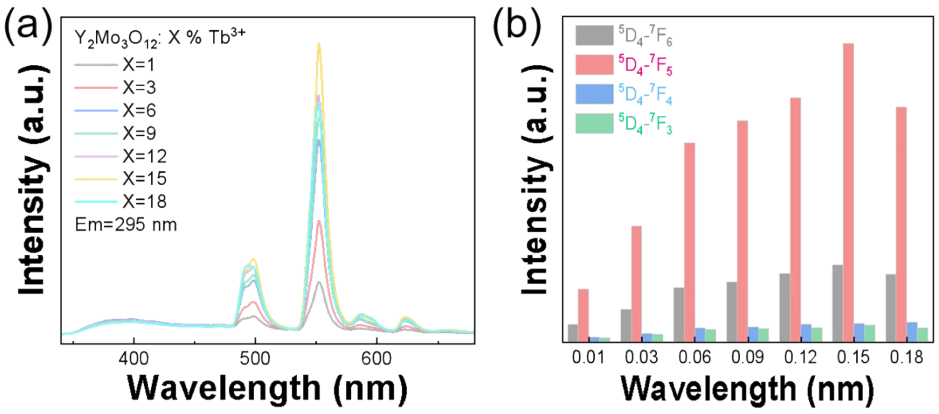

Fig S12. (a) The PL spectra and (b) integrated emission intensity of $Y_2Mo_3O_{12}$: X% Tb^{3+} (X = 0,1,3,6,9,12,15,18) under 295 nm excitation

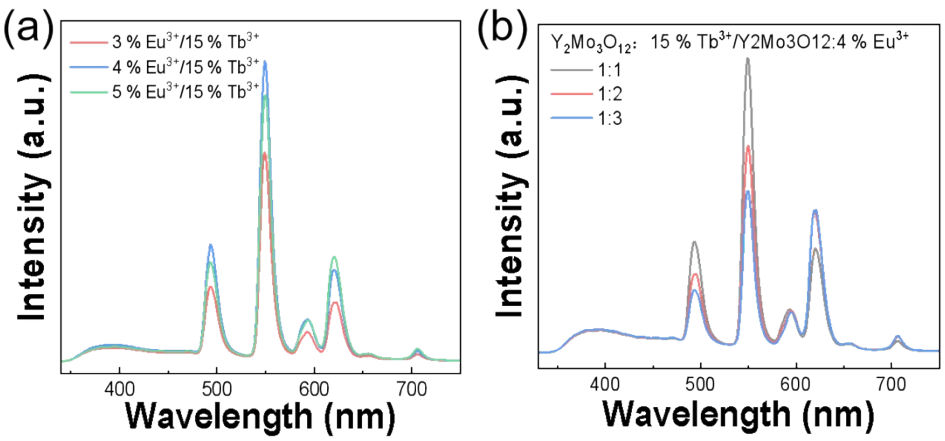

Fig S13.The PL spectrum of (a) $Y_2Mo_3O_{12}$:3%, 4%, 5% Eu^{3+} and $Y_2Mo_3O_{12}$:15% Tb^{3+} mixed phosphor and (b) $Y_2Mo_3O_{12}$:4%Eu^{3+}/15% Tb^{3+} mixed mixed phosphor with different proportions of 1:1, 1:2, 1:3 under 295 nm excitation laser

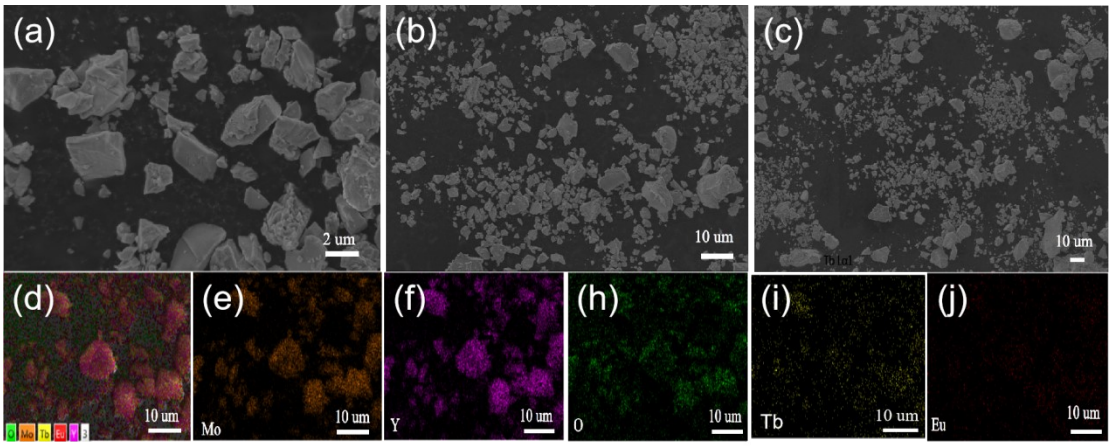

Fig S14. (a-c)The SEM with different magnification ratios of $Y_2Mo_3O_{12}$: 4 % Eu^{3+}/15% Tb^{3+} mixed phosphor; elemental mapping of Mo (e), Y(f), O (h),Tb (i) and Eu (j) elements

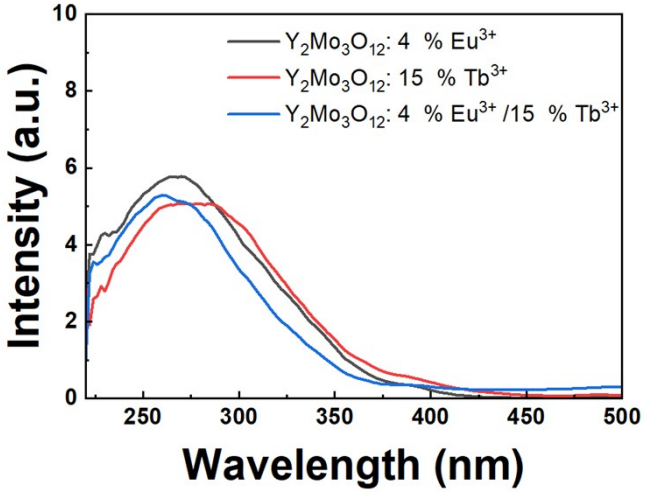

Fig S15. $Y_2Mo_3O_{12}$: 4% Eu^{3+}, $Y_2Mo_3O_{12}$: 15% Tb^{3+} and $Y_2Mo_3O_{12}$: 4% Eu^{3+} / 15 % Tb^{3+} absorption spectra.

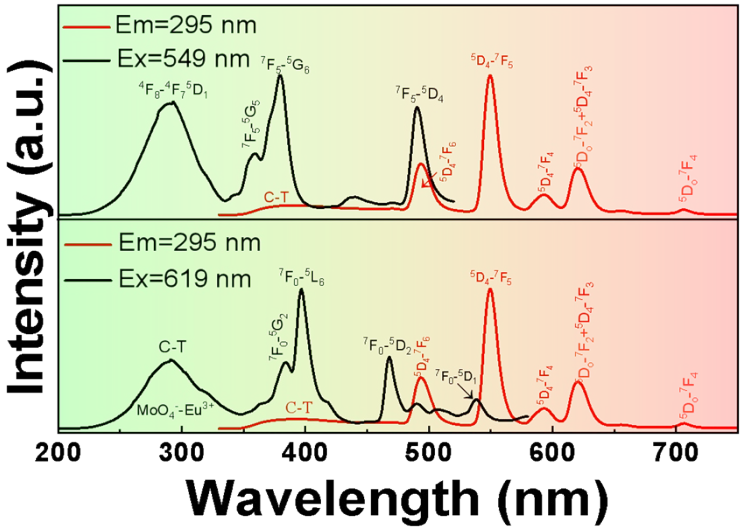

Fig S16. The excitation and emission spectra of $Y_2Mo_3O_{12}$: 4% Eu^{3+}/15% Tb^{3+} mixing phosphor.

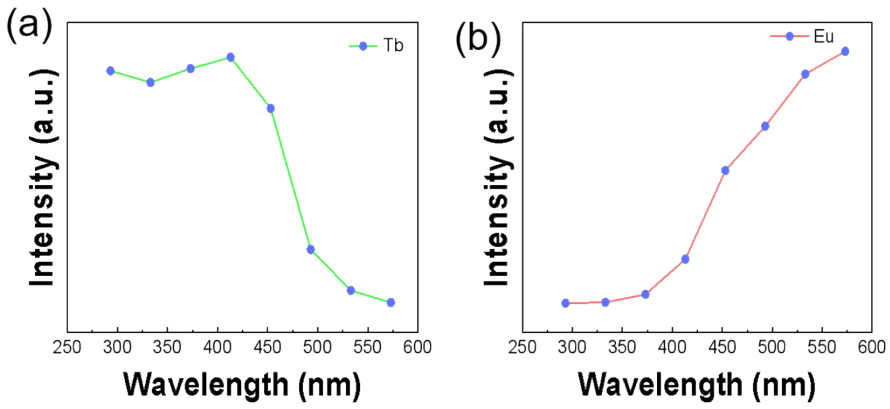

Fig S17. The integrated emission intensity of (a)Tb^{3+} (550 nm) and (b)Eu^{3+} (617 nm) in $Y_2Mo_3O_{12}$: 4% Eu^{3+}/15% Tb^{3+} mixed phosphor under 295 nm excitation at a temperature range of 293-573 K

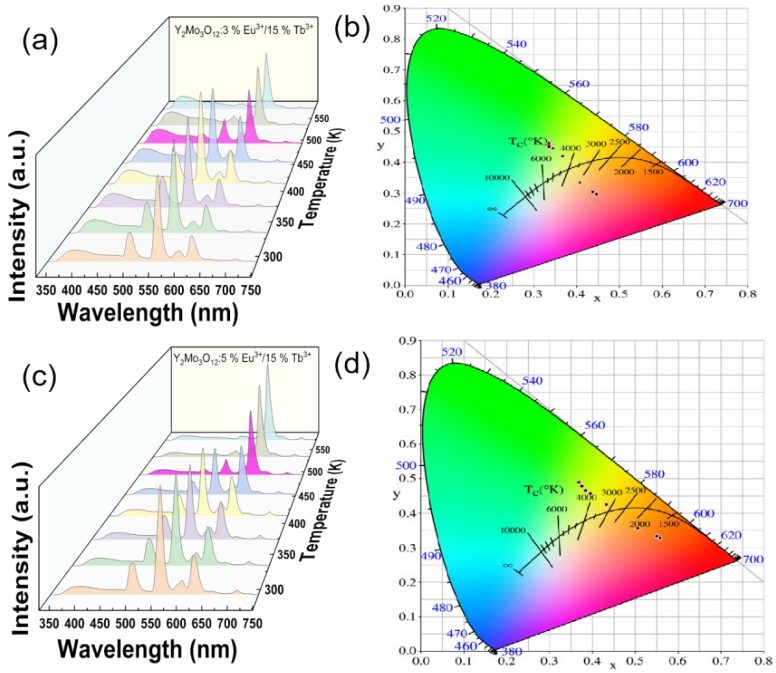

Fig S18. (a) $Y_2Mo_3O_{12}$: 3% Eu^{3+}/15% Tb^{3+} temperature-dependent PL spectra. (b) $Y_2Mo_3O_{12}$: 3% Eu^{3+} /15% Tb^{3+} temperature-dependent CIE coordinates. (c)$Y_2Mo_3O_{12}$: 5% Eu^{3+}/15% Tb^{3+} temperature-dependent PL spectra.(b) $Y_2Mo_3O_{12}$: 5% Eu^{3+}/15% Tb^{3+} temperature-dependent CIE coordinates.

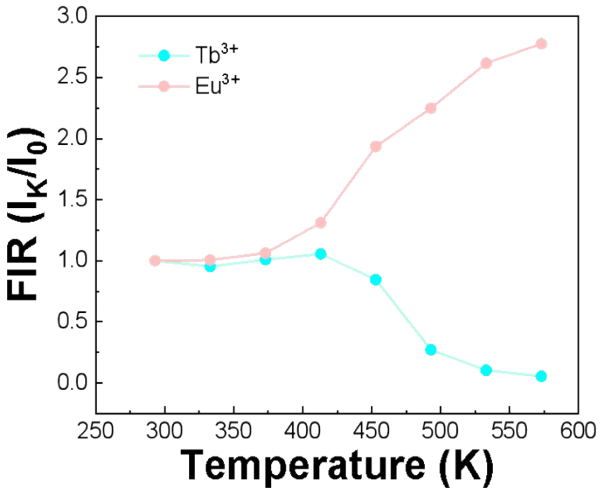

Fig S19. The I_T/I_0 of Tb^{3+} (550 nm) and Eu^{3+}(617 nm) at a temperature range of 293-573 K.

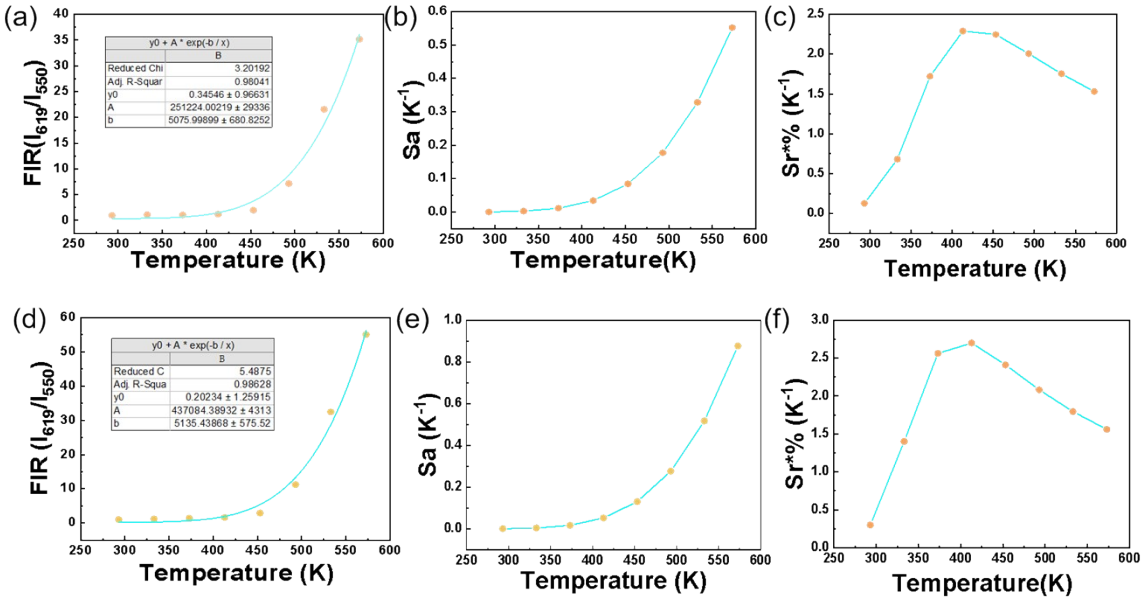

Fig S20. (a-c) The FIR, Sa, Sr of $Y_2Mo_3O_{12}$: 3% Eu^{3+}/15% Tb^{3+} by monitoring Eu (619 nm) and Tb (550 nm). (d-f) The FIR, Sa, Sr of $Y_2Mo_3O_{12}$: 5% Eu^{3+}/15% Tb^{3+} by monitoring Eu (619 nm) and Tb (550 nm).

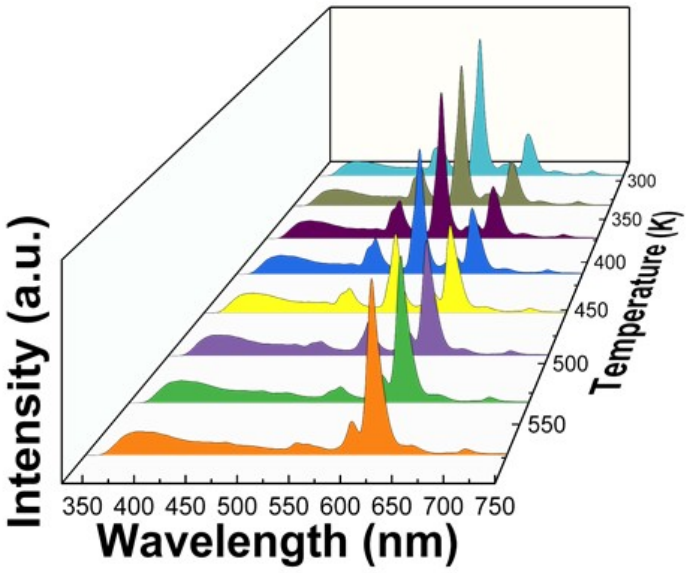

Fig S21. The PL spectra of $Y_2Mo_3O_{12}$: 4% Eu^{3+}/15% Tb^{3+} mixed phosphor during the cooling process.

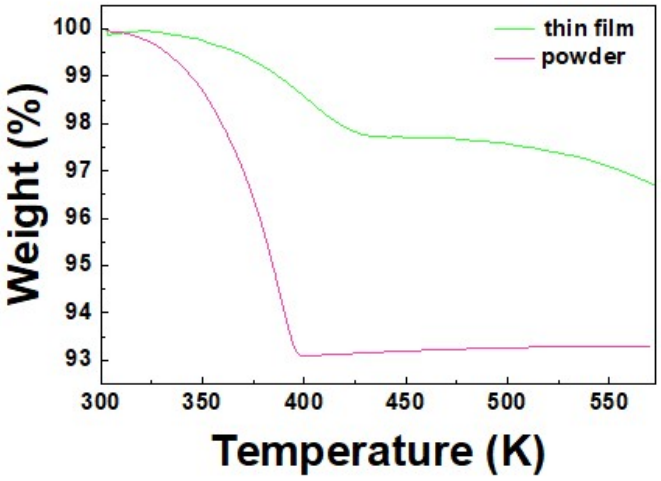

Fig S22. The TG curve of $Y_2Mo_3O_{12}$:Eu^{3+}/Tb^{3+} mixed material and flexible thin

Table S1.The lattice parameters and a/b/c-axis were refined and calculated based on the XRD patterns

Temperature (K)	a(Å)	b(Å)	C(Å)	V
293	13.542	9.843	9.936	1324.611
333	13.503	9.842	9.975	1325.814
373	13.844	9.923	10.023	1377.069
413	13.864	9.928	10.016	1378.854
453	13.867	9.925	10.009	1377.774
493	13.864	9.923	10.009	1377.209
533	13.857	9.916	10.000	1374.304
573	13.847	9.918	9.999	1373.336

Table S2. Comparison of the performance of temperature sensor and visual temperature sensor

Compounds	Temperature (K)	Sr (K^{-1})	References
YBO_3: Bi^{3+}/Eu^{3+}/Tb^{3+}	293−473	0.57%	43
Y_2O_3: Eu^{3+}/ Tb^{3+}	313−513	0.68%	44
Sr_3MoO_6:Eu^{3+}/Tb^{3+}	14−300	0.24%	45
$Sc_2W_3O_{12}$:Eu^{3+}/Tb^{3+}	298−473	2.94%	46
$Gd_2Mo_3O_{12}$:Eu^{3+}/Tb^{3+}	80-450	0.50%	47
$Y_2Mo_3O_{12}$:Eu^{3+}/$Y_2Mo_3O_{12}$:Tb^{3+}	293−573	2.56%	This work

Table S3. The CIE coordinates corresponding to the flexible film at 293 K to 573 K

Temperature (K)	CIE x	CIE y
293	0.349	0.476
333	0.351	0.470
373	0.353	0.469
413	0.365	0.465
453	0.400	0.435
493	0.460	0.351
533	0.499	0.317
573	0.519	0.312